Catalysis Science & Technology

Accepted Manuscript

ROYAL SOCIETY OF CHEMISTRY

www.rsc.org/catalysis

Graphical Abstract

Atmospheric pressure synthesis of nanosized ZSM-5 with enhanced catalytic performance for methanol to aromatics reaction

Kui Shen, Ning Wang, Weizhong Qian, Yu Cui and Fei Wei*

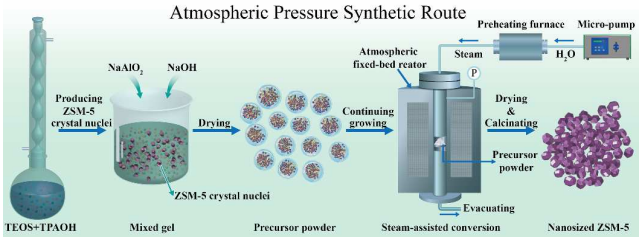

We develop an atmospheric pressure synthetic route for nanosized ZSM-5 with excellent catalytic performance for methanol to aromatics reaction by decoupling its nucleation and growth process. This facile route not only avoids the high hydrothermal pressures and its potential safety concerns, but also could control the crystallization process more flexibly, compared to the conventional hydrothermal route.

Cite this: DOI: 10.1039/c0xx00000x

www.rsc.org/xxxxxx

ARTICLE TYPE

Atmospheric pressure synthesis of nanosized ZSM-5 with enhanced catalytic performance for methanol to aromatics reaction

Kui Shen, Ning Wang, Weizhong Qian,* Yu Cui and Fei Wei

Received (in XXX, XXX) Xth XXXXXXXXX 20XX, Accepted Xth XXXXXXXXX 20XX

DOI: 10.1039/b000000x

We report, for the first time, an atmospheric pressure synthetic route for nanosized ZSM-5 with 100% yield by decoupling its nucleation and growth process. Under unsealed condition, abundant crystal nuclei are first formed in liquid phase and then grow into nanosized ZSM-5 via an improved steam-assisted conversion method using superheated steam as the medium at atmospheric pressure. The obtained nanosized ZSM-5 possesses excellent texture properties, such as high crystallinity, high surface area, tunable Si/Al molar ratio, and uniform size and exhibits far longer lifetime as well as higher selectivity of total aromatics in the catalytic conversion of methanol to aromatics, compared with conventional ZSM-5. This facile route will lead to a very promising future for the large-scale preparation of zeolites with a safe and continuous process under atmospheric pressure.

ZSM-5 zeolite, a crystalline aluminosilicate material with three-dimensional framework and uniform micropores,[1-3] has been widely used as an excellent catalysts for energy chemical industry, due to its unique physicochemical properties, such as high specific surface area, tunable acidity, excellent shape selectivity, and high hydrothermal stability.[4-10] However, the crystallization of ZSM-5 is traditionally conducted hydrothermally with water or other polar solutions as the solvent in a sealed vessel (hydrothermal synthesis reactor) under high autogenous pressure (typically among 8-20 atm),[1, 11-16] which not only give rise to potential security problems and low efficiency, but also increase the difficulty in crystallization control in a solution, where Si or Al species tend to achieve an equilibrium and the nucleation and growth process is difficult to control. To overcome the disadvantages of the hydrothermal method, the use of a dry precursor allows the direct preparation of microporous crystals in the presence of saturated steam, which is called as steam-assisted conversion (SAC) method.[10, 17-24] This method can separate the nucleation and growth process of zeolites, which is beneficial for the facile control of the crystal size.[17, 20, 23] However, the SAC route has similar disadvantages to the hydrothermal route in a sealed condition with high autogenous pressure. Therefore, it remains a great challenge to produce ZSM-5 in a much safety and controllable manner at low cost for several ten years since the invention of ZSM-5.

Recently, Cooper et al. report a new ionothermal approach for the synthesis of zeolite analogues,[25] where ionic liquids act as both solvent and template in an open vessel. This novel method has attracted the interest of many researchers due to the advantages brought about by the simple operating conditions carried out at atmospheric pressure.[26-33] However, the high cost of commonly used ionic liquids, the low yield of zeolites and the very limited solubility of silica precursor materials in the ionic liquids gravely limit the applications of this method to prepare aluminosilicate-based zeolites.[34, 35] In addition, there is still increasing interest on preparing nanosized ZSM-5 considering the necessarity of improving the diffusion ability of crystals for catalytic applications.[9-11] Apparently, it is highly desirable to develop an ambient pressure route for preparing nanosized ZSM-5 with high yield in a much convenient, safe and cheap manner.

Herein, we report an atmospheric pressure route to prepare nanosized ZSM-5 by decoupling its nucleation and growth process. Generally, abundant crystal nuclei are first formed in liquid phase and then grow into nanosized ZSM-5 via an improved steam-assisted conversion under atmospheric pressure. As a result, this facile route not only avoids the high hydrothermal pressures and its potential safety concerns during the entire preparation procedure of ZSM-5, but also could control the crystallization process more flexibly, compared to the hydrothermal route. Moreover, the resultant nanosized ZSM-5 exhibits high crystallinity, tunable Si/Al molar ratio, high surface area, ultrafine uniform size and excellent catalytic performance in the methanol to aromatics reaction (MTA). Furthermore, the modified SAC method greatly increases the crystallization efficiency up to 100 % yield, as well as reducing waste water in large quantities. This facile route represents a great progress in synthesizing ZSM-5 and will be a stimulus to its catalytic applications. And the ideas of decoupling nucleation and growth process would be feasible to the synthesis of other zeolites under ambient pressure.

The preparation of nanosized ZSM-5 under atmospheric pressure is shown schematically in Figure 1a. Briefly, TPAOH and silica source (TEOS) are first mixed and hydrothermally treated at 90 ^{o}C in an opening round-bottom flask. The TEM images of the precursor gel (Figure 1b and 1c) indicate that a few ZSM-5 crystal nuclei with a particle size around 50 nm are produced in this nucleation process. However, the corresponding electron diffraction pattern reveals that the majority of the precursor gel possesses the characteristic of amorphous phase due to the mild crystallization conditions (ambient pressure and low temperature).[36] Then the as-produced crystal nuclei, as well as the unreacted SiO_2 in large amount (Figure 1b and 1c), are mixed

with $NaAlO_2$ and NaOH to become a gel, which is further dried to be precursor powders. In the second step, the unreacted SiO_2 species in dry gel powders are further transformed into ZSM-5 crystals, under the assistance of the already existed ZSM-5 nuclei, in fixed-bed reactor with superheated steam as the medium at 140 ^oC under atmospheric pressure. It is well known that the synthesis of high Al-content nano-ZSM-5 often suffer from many serious problems including very low yield and a tendency for the crystals to agglomerate/intergrow into large particles.[37-40] So, in this contribution, we prepare two nanosized ZSM-5 samples with Si/Al molar ratio of 60 (denoted as ZSM-5-AP60) and 15 (denoted as ZSM-5-AP15), respectively, to certify the much more tunable Si/Al of our route than hydrothermal method.[38-42] The detailed synthesis procedures are better described in the Supporting Information. For comparing the properties of the nanosized ZSM-5, conventional ZSM-5 (Si/Alth=60) is also synthesized according to the modified method reported by JC Groen et al, and its SEM images are shown in Figure S1.[43]

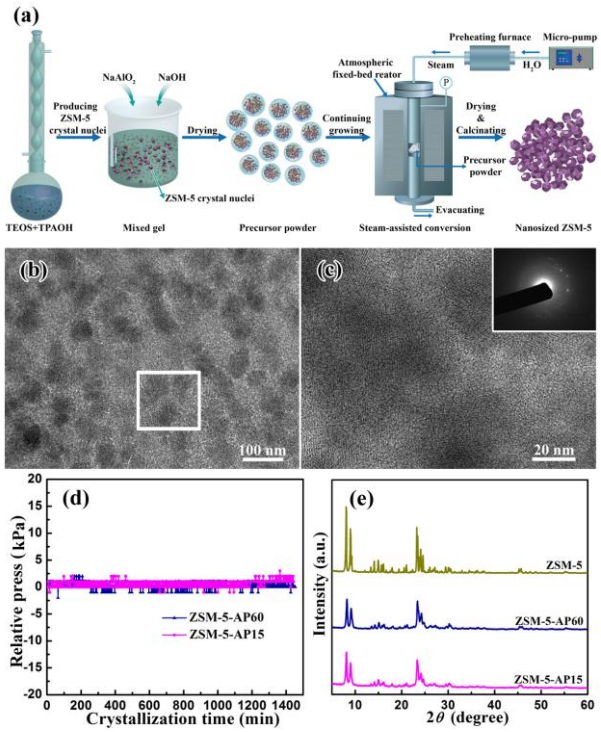

Figure 1 (a) Schematic diagram of the atmospheric pressure synthetic procedures for the nanosized ZSM-5. (b) Low-magnification TEM image and (c) High-magnification TEM images of the precursor gel (The inset is its corresponding electron diffraction pattern). (d) monitored pressure curves of ZSM-5-AP15 and ZSM-5-AP60 as a function of crystallization time at 140 ^oC. (e) XRD patterns of ZSM-5-AP15 and ZSM-5-AP60 and conventional ZSM-5.

We monitor the pressure changes of the fixed-bed reactor in the synthesis process of ZSM-5-AP15 and ZSM-5-AP60. The monitored pressure curves are given in Figure 1d, which directly indicate that the whole crystallization process is completed at ambient pressure since the pressure is always fluctuated at ambient pressure. The XRD patterns (Figure 1e) of both conventional and nanosized ZSM-5 prepared under crystallization temperature of 140 ^oC (see supporting information) show five well-resolved peaks at 7.98 °, 8.82 °, 23.18 °, 24.02 ° and 24.46, which are in good agreement with high crystalline MFI-structured ZSM-5 without any impurities or amorphous phase.[8, 44] It is noteworthy that the XRD line widths of ZSM-5-AP15 and ZSM-5-AP60 are much broader than those for conventional ZSM-5, which is due to their smaller crystal size as compared with conventional ZSM-5 according to the Scherrer equation. In addition, the UV-Raman spectra of all samples show a wide band at 380 cm^{-1} (Figure S2), which is associated with the framework symmetric stretching vibration of a five-membered building unit in ZSM-5.[10, 45, 46] However, the sample prepared by crystallizing directly in the ambient fixed-bed reactor, in the absence of gel seeds, exhibits the features of a major amorphous phase plus a MFI-structured ZSM-5 phase with low crystallinity (Figure S3 and S4). The comparison indicates that the first nucleation step in Figure1a plays a dominant role in eliminating the maximal crystallization barrier, which is crucial to second full crystallization step in ambient pressure.

SEM and TEM images of ZSM-5-AP15 and ZSM-5-AP60 are shown in Figures 2a-2f, which clearly show that both samples are composed of monodispersed ZSM-5 particles with uniform sizes of about 60 nm, which is comparable to the smallest one prepared by conventional hydrothermal method.[37-40] The atmospheric pressure synthetic route includes an nucleation process before the improved stream-assisted crystallization, which is considered to produce abundant ZSM-5 nuclei (Figure 1), leading to the formation of the small and uniform nanosized ZSM-5. Analysis with higher-magnification TEM images (Figure 2e and 2f) reveals that all the particles are completely crystalline, as the parallel lattice fringes can be clearly observed and spread throughout the specimen. The corresponding selected area electron diffractions (Figure 2e inset and 2f inset) indicate that every individual particle is a ZSM-5 single crystal, exhibiting a single diffraction pattern.[6, 8, 10] The absence of sponge-like material in the SEM and TEM pictures indicates the absence of amorphous material, in agreement with XRD characterization. Since no silica and aluminum source are washed away in the whole synthetic route, the yield of these nanosized ZSM-5 is nearly 100%, which is in stark contrast to the low yields of nanoparticles usually obtained from conventional hydrothermal route.[37-40] The high yield of our route is probably due to the uneasy revisable migration of Al and Si species out of the framework, as compared to that in hydrothermal condition, where the Si and Al species tend to achieve equilibrium in a solution. Therefore, we, for the first time, validate that the crystallization of ZSM-5 is completely done at ambient pressure using our route, which is similar to the conventional SAC method operated at high pressure. In addition, we have prepared another nano-ZSM-5 sample with an Si/Al of infinite (denoted as N-Silicalite-1, Figure S5) by atmospheric pressure synthesis route. It's worth noting that the size and morphology of the final products is nearly independent of the Si/Al ratio of the ZSM-5 precursor, indicating the improved SAC step provides great flexibility to prepare uniform nanosized ZSM-5 with a broad Si/Al ratio and tunable acidity.

The nitrogen adsorption/desorption isotherms and BJH pore size distribution demonstrate the substantial mesoporous network of the both nanosized ZSM-5. As shown in Figure 3a, the nitrogen adsorption isotherms of ZSM-5-AP15 and ZSM-5-AP60 show a typical type-I curve plus type-IV curve with a sharp uptake and an obvious hysteresis loop at the high relative pressure range of 0.8 to1, which is indicative of its remarkable micro-/mesoporous structure.[47, 48] Unlike the nanosized ZSM-5,

the conventional ZSM-5 shows a typical type-I isotherm corresponding to the solely microporous structure. According to

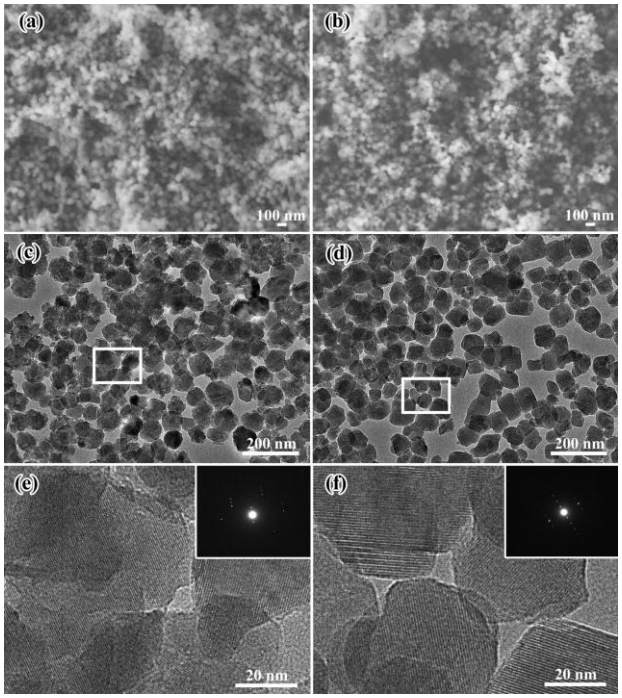

Figure 2 SEM images of (a) ZSM-5-AP15 and (b) ZSM-5-AP60. TEM images of (c) ZSM-5-AP15, and (d) ZSM-5-AP60 and HR-TEM images of (e) ZSM-5-AP15 and (f) ZSM-5-AP60 taken from the square frame in (c) and (d), respectively. (The inset is its corresponding electron diffraction pattern).

pore size analysis by the BJH method using the adsorption isotherm, the mesopore diameters in both nanosized ZSM-5 have a broad distribution centered on 25 nm, which belongs to the stacking intercrystalline mesopores of nanosized ZSM-5. Correspondingly, the nanosized ZSM-5 have a much higher BET area and a larger total pore volume (above 400 m^2 g^{-1} and 0.61 cm^3 g^{-1}) compared to those of conventional ZSM-5 (357 m^2 g^{-1} and 0.17 cm^3 g^{-1}) (Table S1). It is well known that the framework Al of ZSM-5 may function either as active sites or as anchoring points for catalytic sites. Thus, we perform ^{27}Al MAS NMR spectroscopy to acquire the coordination environment of aluminum atoms in ZSM-5-AP15 and ZSM-5-AP60. As shown in Figure 3b, ^{27}Al MAS-NMR spectra of the three samples show one sharp aluminum peak at 52 ppm, which can be assigned to aluminum species with tetrahedral coordination environment. Furthermore, no signal at 0 ppm is detected, indicating that the Al atoms are entirely incorporated into the crystalline frameworks of the nanosized ZSM-5.[49]

The crystallization curves (Figure 3c) derived from XRD patterns (Figure S6) indicate that the amorphous phase could completely convert to high crystallized nanosized ZSM-5 just within 12 h because of the present of ZSM-5 nuclei formed in the first step (Figure 1b and 1c), which eliminates the most time-consuming nucleation process. It is also worth noting that the Al content of the ZSM-5 precursor could not affect crystallization rate, which is different from the general pattern when using hydrothermal methods.[40] It is well known that TPAOH is the most common SDAs for ZSM-5 synthesis.[8, 14-16, 23, 24] When being used, such a non-volatile SDA can be involved in a dry gel.[23, 24] TG analysis of the dry precursor suggests that the TPAOH in dry gel precursor could be decomposed at above 150 °C (Figure S7). It allows us to understand the effect of the crystallization

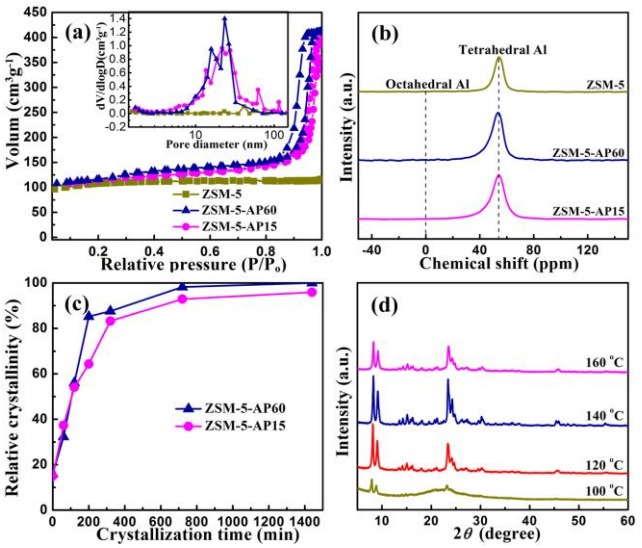

Figure 3 (a) Nitrogen adsorption/desorption isotherms and BJH pore size distribution based on the adsorption isotherm (inset) for nanosized ZSM-5 and conventional ZSM-5. (b) 27Al-NMR spectra of nanosized ZSM-5 and conventional ZSM-5. (c) Crystallization curves of ZSM-5-AP15 and ZSM-5-AP60 via dry-gel conversion at 140 °C. (d) XRD patterns of the products prepared by atmospheric pressure synthetic route at different crystallization temperature.

temperature on the crystallization process. As shown in Figure 3d, the sample prepared at 140 °C shows the highest crystallinity among all samples. Apparent, lower crystallization temperature could not drive the condensation reactions between soluble silicate and aluminate ions, restraining the growth process of the ZSM-5 crystals.[50, 51] On the other hand, higher crystallization temperature will not only lead to the decomposition of the template, but also rapidly decreases the relative humidity of steam in the reactor, which strongly influence the crystallinity of the final product.[21]

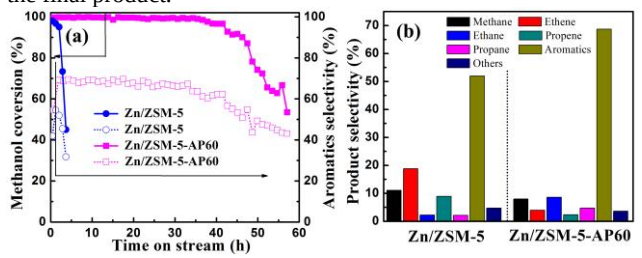

Figure 4 (a) Methanol conversions and total aromatics selectivity over Zn/ZSM-5-AP60 and conventional Zn/ZSM-5 as a function of time-on-stream (reaction temperature: 475 °C, WHSV: 0.75 h^{-1}, The solid and open curves are the methanol conversions and total aromatics selectivity, respectively), (b) product selectivity of MTA reactions over Zn/ZSM-5-AP60 and conventional Zn/ZSM-5 after the reactions being stable (the date are obtained for the ZSM-5-AP60 and the conventional ZSM-5 at 3.1h and 1.2h time on stream, respectively).

The actual Si/Al_{ICP} molar ratios of ZSM-5-AP15 and ZSM-5-AP60 are 16.2 and 67.9, respectively (Table S1). Both the NH_3-TPD profiles (Figure S8) and pyridine-adsorbed FTIR spectra (Figure S9) show that the strength and types of acid sites for

ZSM-5-AP60 and conventional ZSM-5 (Si/Al_{ICP}=77, Table S1) are almost identical. However, the ZSM-5-AP15 show much more concentrated acid site than ZSM-5-AP60 and conventional ZSM-5 due to its high framework Al content. In order to investigate the catalytic activity of meso-/macroporous structure, the MTA reaction are carried out over Zn/ZSM-5-AP60 and conventional Zn/ZSM-5 using a stainless steel fixed bed. As shown in Figure 4a, the Zn/ZSM-5-AP60 exhibits a high methanol conversion (above 96%) with a total aromatics selectivity of above 62% during the incipient 42 h time on stream. For comparison, the initial methanol conversion of conventional Zn/ZSM-5 can also reach 98% but shows the rapid decline just within 3.6 h testing time at such a strict reaction condition. Furthermore, the total aromatic selectivity for the conventional Zn/ZSM-5 is much lower (below 54%) than that for Zn/ZSM-5-AP60. Considering the similarities of ZSM-5-AP60 and conventional ZSM-5 in terms of Si/Al_{ICP} molar ratio, acidity and micropore volume (Table S1, Figure S8 and S9), the superior catalytic performance over Zn/ZSM-5-AP60 compared to that over conventional Zn/ZSM-5 could be directly attributed to the small size of the nanosized ZSM-5, which favours the diffusion of reactants/products and thus prevent the deposition of coking precursor. As we all known, the relatively small pore size of conventional ZSM-5 often results in unacceptably slow diffusion of methanol and aromatics from the active sites located inside the zeolite crystals, leading to the lower aromatics selectivity and shorter lifetime in MTA process, when compared with nanosized ZSM-5. Actually, TG profiles (Figure S10) clearly show the coke formation rate over Zn/ ZSM-5-AP60 is about 4.41 mg $g_{cat}^{-1}h^{-1}$, which is much lower than that over conventional Zn/ZSM-5 (26.33 mg g_{cat}^{-1} h^{-1}). In addition, detailed product selectivities after the reactions being stable are also given in Figure 4b. The Zn/ZSM-5-AP60 show lower overall olefin selectivity than conventional Zn/ZSM-5, possibly caused by its enhanced hydrogen transfer capability to produce more aromatics.[52] These reaction results show that the highly mesoporous nanosized ZSM-5 obtained by atmospheric pressure synthetic route is expected to be an excellent catalyst for MTA reactions and other bulky-molecule involved reactions of industrial importance.

In summary, we have developed a facile route to prepare nanosized ZSM-5 under atmospheric pressure by decoupling its nuclea-tion and growth process. The first step of forming a few ZSM-5 crystal nuclei in liquid phase and the second step to grow nanosized ZSM-5 from precursor under superheated steam are both carried out under ambient pressure. We evidenced that the formation of some ZSM-5 nuclei in the first step eliminates the maximal crystallization barrier and is essential for the downstream crystallization. This facile route not only avoids the high hydrothermal pressures and its potential safety concerns, but also could control the crystallization process more flexibly. Moreover, the resultant nanosized ZSM-5 possesses excellent texture properties and catalytic performance for the methanol to aromatics (MTA) reaction, compared with conventional ZSM-5. Taking all of these features into account, it is believable that this facile route will lead to a very promising future for the large-scale preparation of zeolite-based catalysts with a safe and continuous process under atmospheric pressure condition.

Notes and references

Beijing Key Laboratory of Green Chemical Reaction Engineering and Technology, Department of Chemical Engineering,Tsinghua University, Beijing 100084, PR China, E-mail: qianwz@ tsinghua.edu.cn; Fax: +86 10 6277 2051; Tel: +86 10 6279 4133

† Electronic Supplementary Information (ESI) available: [details of any supplementary information available should be included here]. See DOI: 10.1039/b000000x/

‡ Footnotes should appear here. These might include comments relevant to but not central to the matter under discussion, limited experimental and spectral data, and crystallographic data.

1. G. Kokotailo, S. Lawton and D. Olson, *Nature*, 1978, **272**, 437-438.
2. D. Olson, G. Kokotailo, S. Lawton and W. Meier, *J. Phys. Chem.*, 1981, **85**, 2238-2243.
3. M. B. Roeffaers, R. Ameloot, M. Baruah, H. Uji-i, M. Bulut, G. De Cremer, U. Müller, P. A. Jacobs, J. Hofkens and B. F. Sels, *J. Am. Chem. Soc.*, 2008, **130**, 5763-5772.
4. C. S. Cundy and P. A. Cox, *Chem. Rev.*, 2003, **103**, 663-702.
5. C. H. Christensen, K. Johannsen, I. Schmidt and C. H. Christensen, *J. Am. Chem. Soc.*, 2003, **125**, 13370-13371.
6. Z. Lai, G. Bonilla, I. Diaz, J. G. Nery, K. Sujaoti, M. A. Amat, E. Kokkoli, O. Terasaki, R. W. Thompson and M. Tsapatsis, *Science*, 2003, **300**, 456-460.
7. A. Corma, *Chem. Rev.*, 1997, **97**, 2373-2420.
8. F. Liu, T. Willhammar, L. Wang, L. Zhu, Q. Sun, X. Meng, W. Carrillo-Cabrera, X. Zou and F.-S. Xiao, *J. Am. Chem. Soc.*, 2012, **134**, 4557-4560.
9. K. Shen, W. Qian, N. Wang, J. Zhang and F. Wei, *J. Mater. Chem. A*, 2013, **1**, 3272-3275.
10. K. Shen, W. Qian, N. Wang, C. Su and F. Wei, *J. Am. Chem. Soc.*, 2013, **135**, 15322-15325.
11. M. Choi, H. S. Cho, R. Srivastava, C. Venkatesan, D.-H. Choi and R. Ryoo, *Nat. Mater.*, 2006, **5**, 718-723.
12. M. Choi, K. Na, J. Kim, Y. Sakamoto, O. Terasaki and R. Ryoo, *Nature*, 2009, **461**, 246-249.
13. K. Na, C. Jo, J. Kim, K. Cho, J. Jung, Y. Seo, R. J. Messinger, B. F. Chmelka and R. Ryoo, *Science*, 2011, **333**, 328-332.
14. W. Fan, M. A. Snyder, S. Kumar, P.-S. Lee, W. C. Yoo, A. V. McCormick, R. L. Penn, A. Stein and M. Tsapatsis, *Nat. Mater.*, 2008, **7**, 984-991.
15. P.-S. Lee, X. Zhang, J. A. Stoeger, A. Malek, W. Fan, S. Kumar, W. C. Yoo, S. Al Hashimi, R. L. Penn and A. Stein, *J. Am. Chem. Soc.*, 2010, **133**, 493-502.
16. W. C. Yoo, S. Kumar, R. L. Penn, M. Tsapatsis and A. Stein, *J. Am. Chem. Soc.*, 2009, **131**, 12377-12383.
17. G. Majano, S. Mintova, O. Ovsitser, B. Mihailova and T. Bein, *Microporous Mesoporous Mater.*, 2005, **80**, 227-235.
18. F. Taborda, Z. Wang, T. Willhammar, C. Montes and X. Zou, *Microporous Mesoporous Mater.*, 2012, **150**, 38-46.
19. S. Inagaki, K. Nakatsuyama, Y. Saka, E. Kikuchi, S. Kohara and M. Matsukata, *J. Phys. Chem. C*, 2007, **111**, 10285-10293.
20. K. Möller, B. Yilmaz, R. M. Jacubinas, U. Müller and T. Bein, *J. Am. Chem. Soc.*, 2011, **133**, 5284-5295.
21. S. P. Naik, A. S. Chiang and R. Thompson, *J. Phys. Chem. B*, 2003, **107**, 7006-7014.
22. J. Yao, H. Wang, S. P. Ringer, K.-Y. Chan, L. Zhang and N. Xu, *Microporous Mesoporous Mater.*, 2005, **85**, 267-272.
23. K. Zhu, J. Sun, J. Liu, L. Wang, H. Wan, J. Hu, Y. Wang, C. H. Peden and Z. Nie, *ACS Catal.*, 2011, **1**, 682-690.

24. N. Ren, B. Subotić, J. Bronić, Y. Tang, M. Dutour Sikirić, T. Mišić, V. Svetličić, S. Bosnar and T. Antonić Jelić, *Chem. mater.*, 2012, **24**, 1726-1737.
25. E. R. Cooper, C. D. Andrews, P. S. Wheatley, P. B. Webb, P. Wormald and R. E. Morris, *Nature*, 2004, **430**, 1012-1016.
26. E. R. Parnham and R. E. Morris, *Chem. mater.*, 2006, **18**, 4882-4887.
27. E. R. Parnham and R. E. Morris, *Acc. Chem. Res.*, 2007, **40**, 1005-1013.
28. E. R. Parnham and R. E. Morris, *J. Am. Chem. Soc.*, 2006, **128**, 2204-2205.
29. E. R. Parnham, P. S. Wheatley and R. E. Morris, *Chem. comm.*, 2006, 380-382.
30. R. Cai, M. Sun, Z. Chen, R. Munoz, C. O'Neill, D. E. Beving and Y. Yan, *Angew. Chem. Int. Ed.*, 2008, **47**, 525-528.
31. H. Ma, R. Xu, W. You, G. Wen, S. Wang, Y. Xu, B. Wang, L. Wang, Y. Wei and Y. Xu, *Microporous Mesoporous Mater.*, 2009, **120**, 278-284.
32. H. Ma, Z. Tian, R. Xu, B. Wang, Y. Wei, L. Wang, Y. Xu, W. Zhang and L. Lin, *J. Am. Chem. Soc.*, 2008, **130**, 8120-8121.
33. K. Li, Z. Tian, X. Li, R. Xu, Y. Xu, L. Wang, H. Ma, B. Wang and L. Lin, *Angew. Chem. Int. Ed.*, 2012, **51**, 4397-4400.
34. P. S. Wheatley, P. K. Allan, S. J. Teat, S. E. Ashbrook and R. E. Morris, *Chem. Sci.*, 2010, **1**, 483-487.
35. R. Cai, Y. Liu, S. Gu and Y. Yan, *J. Am. Chem. Soc.*, 2010, **132**, 12776-12777.
36 H. Mochizuki, T. Yokoi, H. Imai, R. Watanabe, S. Namba, J. N. Kondo and T. Tatsumi, *Microporous Mesoporous Mater.*, 2011, **145**, 165-171.
37. W. Song, V. Grassian and S. Larsen, *Chem. comm.*, 2005, 2951-2953.
38. S. C. Larsen, *J. Phys. Chem. C*, 2007, **111**, 18464-18474.
39. R. Van Grieken, J. Sotelo, J. Menendez and J. Melero, *Microporous Mesoporous Mater.*, 2000, **39**, 135-147.
40. V. B. Mortola, A. P. Ferreira, J. M. Fedeyko, C. Downing, J. M. Bueno, M. C. Kung and H. H. Kung, *J. Mater. Chem.*, 2010, **20**, 7517-7525.
41. W. Song, R. Justice, C. Jones, V. Grassian and S. Larsen, *Langmuir*, 2004, **20**, 8301-8306.
42. T. Xue, Y. M. Wang and M.-Y. He, *Microporous Mesoporous Mater.*, 2012, **156**, 29-35.
43 J. C. Groen, T. Bach, U. Ziese, A. M. Paulaime-van Donk, K. P. de Jong, J. A. Moulijn and J. Pérez-Ramírez, *J. Am. Chem. Soc.*, **2005**, 127, 10792-10793.
44. Y.-Q. Deng, S.-F. Yin and C.-T. Au, *Ind. Eng. Chem. Res.*, 2012, **51**, 9492-9499.
45. Y. Yu, G. Xiong, C. Li and F.-S. Xiao, *J. Catal.*, 2000, **194**, 487-490.
46. L. Ren, Q. Wu, C. Yang, L. Zhu, C. Li, P. Zhang, H. Zhang, X. Meng and F.-S. Xiao, *J. Am. Chem. Soc.*, 2012, **134**, 15173-15176.
47. M. Imperor-Clerc, P. Davidson and A. Davidson, *J. Am. Chem. Soc.*, 2000, **122**, 11925-11933.
48. X. Liu, B. Tian, C. Yu, F. Gao, S. Xie, B. Tu, R. Che, L. M. Peng and D. Zhao, *Angew. Chem. Int. Ed.*, 2002, **41**, 3876-3878.
49. T.-O. Do, A. Nossov, M.-A. Springuel-Huet, C. Schneider, J. L. Bretherton, C. A. Fyfe and S. Kaliaguine, *J. Am. Chem. Soc.*, 2004, **126**, 14324-14325.
50. G. J. d. A. Soler-Illia, C. Sanchez, B. Lebeau and J. Patarin, *Chem. Rev.*, 2002, **102**, 4093-4138.
51. J. Aguado, D. Serrano and J. Rodriguez, *Microporous Mesoporous Mater.*, 2004, **75**, 41-49.
52. P. Sazama, B. Wichterlova, J. Dedecek, Z. Tvaruzkova, Z. Musilova, L. Palumbo, S. Sklenak and O. Gonsiorova, *Microporous Mesoporous Mater.*, 2011, **143**, 87-96.